PNAS Nexus, 2024, 3, pgae213
https://doi.org/10.1093/pnasnexus/pgae213
Advance access publication 30 May 2024
Research Report

A biospecies-derived genomic DNA hybrid gel electrolyte for electrochemical energy storage

Sekhar Babu Mitta[a,*], Jeonghun Kim[a], Harpalsinh H. Rana[b], Samanth Kokkiligadda[c], Yong Taik Lim[c], Suk Ho Bhang[c], Ho Seok Park[c] and Soong Ho Um[a,c,*]

[a]Progeneer Inc., #1002, 12, Digital-ro 31-gil, Guro-gu, Seoul 08380, South Korea
[b]Laboratory of Electrochemistry and Physicochemistry of Materials & Interfaces (LEPMI), CNRS/Grenoble-INP/UGA 1130, Rue de la Piscine, 38402 Saint-Martin d'Heres Cedex, France
[c]School of Chemical Engineering, Sungkyunkwan University, 2066 Seobu-ro, Jangan-gu, Suwon-si, Gyeonggi-do 16419, South Korea
*To whom correspondence should be addressed: Emails: sekharbabu@progeneer.com or sekhar208@gmail.com; sh.um@skku.edu
Edited By: Derek Abbott

Abstract

Intrinsic impediments, namely weak mechanical strength, low ionic conductivity, low electrochemical performance, and stability have largely inhibited beyond practical applications of hydrogels in electronic devices and remains as a significant challenge in the scientific world. Here, we report a biospecies-derived genomic DNA hybrid gel electrolyte with many synergistic effects, including robust mechanical properties (mechanical strength and elongation of 6.98 MPa and 997.42%, respectively) and ion migration channels, which consequently demonstrated high ionic conductivity (73.27 mS/cm) and superior electrochemical stability (1.64 V). Notably, when applied to a supercapacitor the hybrid gel-based devices exhibit a specific capacitance of 425 F/g. Furthermore, it maintained rapid charging/discharging with a capacitance retention rate of 93.8% after ∼200,000 cycles while exhibiting a maximum energy density of 35.07 Wh/kg and a maximum power density of 193.9 kW/kg. This represents the best value among the current supercapacitors and can be immediately applied to minicars, solar cells, and LED lightning. The widespread use of DNA gel electrolytes will revolutionize human efforts to industrialize high-performance green energy.

Keywords: genomic DNA, electrolyte, supercapacitor, flexibility, biospecies

Significance Statement

Design parameters defined in recent years to create better environment-friendly electrical storage should embed as much electrical energy as possible in small, lightweight, and portable packages. For this purpose, it is essential to develop a electrolyte that efficiently captures and transports metal ions and excellent connectivity to either electrodes. This work synthesizes a biospecies genomic DNA hybrid gel electrolyte because of simple combination processing. Surprisingly, it significantly improves electrical energy efficiency. When applied to a supercapacitor, it is easy to transfer ions to the electrode, so that charging and discharging can be performed at a faster speed, thereby simplifying the electric circuit and reducing costs. It also allows the manufacture of thin, lightweight, and miniaturized devices.

Introduction

The escalating demand for advanced energy storage devices underscores the need for materials that combine high-performance with environmental sustainability. Extending the energy-driven principles of living organisms or their components that rely on biological materials into the electrical industry can be beneficial to generate new electrolytes (1–3). DNA, the hereditary material present in living organisms, possesses unique structural, electrochemical, and self-assembly properties that are highly desirable for energy storage applications (4). Moreover, DNA's compatibility with a variety of chemical modifications allows for the integration of other functional materials, leading to hybrid systems with enhanced properties. DNA-based hybrid hydrogel electrolytes represent a groundbreaking class of materials, harnessing the unique molecular recognition capabilities of DNA to create precise and tunable structures (5). This novel material

Competing Interest: S.B.M. and S.H.U. are inventors on patents related to DNA hydrogel electrolyte. These patents have been licensed to Progeneer Incorporated (KR 10-2023-0050492 and PCT/KR2023/005250). The study is being jointly researched and developed for commercialization under a confidentiality agreement between the Progeneer Inc. and the Samsung Advanced Institute of Technology (SAIT). The remaining authors declare no competing interests.
Received: January 25, 2024. **Accepted:** May 21, 2024

has emerged as promising candidates due to their unique physical properties and functional versatility which offers significant potential for enhancing the performance and functionality of energy storage devices (6).

The electrolytes currently in use are considerably limited due to their low flexibility, high fire risk, inefficient mass production processes, and environmental pollution from uncontrolled disposal (7–9). However, the electrolytes in biological systems are nontoxic, chemically stable, exhibit good ionic conductivity, and provide excellent energy storage performance (10–12). The gel polymer electrolytes (GPEs), such as hydrogels, zwitterionic gels, and ionogels, are immobilized liquid electrolytes in a polymer matrix acting concurrently as electrolyte and separator with reduced risk of leakage and evaporation (3, 13). However, the environmental impact of conventional hydrogels, which are often nonbiodegradable, poses a significant challenge, especially in the context of global waste management issues. In response to this, the development of biodegradable hybrid hydrogels has gained momentum. These hydrogels not only retain the advantageous characteristics of traditional hydrogels, such as high ionic conductivity and mechanical flexibility, but also offer an eco-friendly alternative by being compostable and derived from renewable resources (2, 14, 15). This aligns with the growing emphasis on developing materials that reduce the ecological footprint of energy storage systems.

A facile and rapid synthesis approach for hybrid hydrogel networks with significant mechanical strength and high ionic conductivity remains to be addressed. Owing to the fact that metal ions have high affinity towards DNA phosphate groups along their backbone, they can effectively interfere with electron transport under physiological pH (16–19). This characteristic property can be leveraged in electrolyte development and has been utilized in electrochemical energy storage applications such as supercapacitors (20). Here, we propose a free-standing large-area hybrid hydrogel demonstrated from DNA (extracted from fish, chicken, and human) and various polysaccharides (agarose, alginate, and lignin) through electrostatic coupling and proving its applicability as a high-performance supercapacitor. The DNA hybrid hydrogels unveiled its stable polymer network with excellent mechanical integrity, high porosity, and interconnected pore structures which ensures efficient ion transport throughout the gel demonstrating high ionic conductivity of 73.27 mS/cm. These hybrid gels harness the synergistic properties of both components, paving the way for innovative energy storage devices that exhibit a maximum specific capacitance of 425 F/g. Integration and utilization of DNA with other biopolymers lower the overall cost of DNA with a synergistic effect highlighting our uniqueness. Comparatively, the overall electrochemical performances (specific capacitance, device stability, and efficiency) of DNA-hybrid gels were significantly enhanced and have a broad prospect in emerging energy storage technologies that harmonize technological advancement with environmental stewardship.

Results

According to the International Union for Conservation of Nature and Natural Resources (IUCN) 2007 Red List, fish and birds account for 66.8% of the readily available fauna. Salmon, which can be used immediately without processing, was employed in the proof-of-concept model in this study. Here, the usage of DNA from species such as salmon fish is elaborated with the concept of employing waste or byproducts from the fish industry. The fish processing industry yields a significant amount of waste, along with parts like skin, bones, heads, and milt (sperm). Many researchers have been investigating the potential value of these byproducts for applications such as in the cosmetic industry, biomedical, and photonic devices that have been studied using salmon sperm DNA. Utilizing waste from the fish industry, like salmon sperm DNA, not only adds value to the industry but also helps in lowering the environmental impact of waste. With renewed research, there is potential for even more advanced applications of these byproducts in the future. Genes contained in sperm heaps or blood discarded after spawning were used directly. They were mixed with the most commonly used lithium metal ions and simply prepared as an electrolyte. Figure 1a illustrates the scheme of DNA extraction from salmon fish and birds, gel electrolyte processes, and application in electrical storage in vehicles and lighting LED bulbs. The salmon sperm DNA fibers made an amorphous gel by adding the required concentration of lithium chloride (LiCl) salts and repeating heating and cooling (20). LiCl is employed in preparing DNA hydrogels due to their unique physicochemical properties, which significantly influence the interactions between DNA molecules. A few such properties are capable of enhancing DNA solubility, stabilizing DNA structures through specific interactions (lithium ions binding to phosphate groups of DNA), improving physical properties (mechanical strength and swelling behavior) of DNA hydrogels, increasing ionic conductivity and thermal stability. Generally, LiCl has a relatively high lattice energy owing to their strong electrostatic attraction between Li^+ and Cl^- which might significantly influence the properties of host material when doped. The high lattice energy indicates that LiCl readily dissociates into ions which contribute to improve the ionic conductivity.

To determine the optimum amount of LiCl, concentration-dependent impedance analysis of the DNA gel electrolyte was performed (Fig. 1b–d) through electrochemical impedance spectroscopy (EIS). The DNA gel electrolytes were prepared with various LiCl concentrations of 10, 50, 100, 200, 500, and 800 mM. The comparative analysis of electrical conductivity showed that the conductivity increased as the concentration of LiCl increased to approximately 200 mM and as soon as more ions were added, the electrical conductivity gradually decreased due to the salt flocculation effect. Ion transport processes have been studied using temperature-dependent ionic conductivity of DNA gel electrolytes at temperatures ranging from 30 to 60°C as illustrated in Fig. 1e–g. The $\ln \sigma$ vs. 1000/T plot was almost linear ($R^2 = 0.991$), indicating that the conductivity of DNA gel electrolytes obeys the Arrhenius equation used to estimate the activation energy (E_a) to be 0.04 eV. Thus, this suggests that ion transport was primarily driven by the diffusion of thermally activated ions through the channels in the physically intertwined DNA gel networks. Meanwhile, the relatively small, highly concentrated Li^+ with better ion binding capacity takes up space by replacing the existing sodium ions in the DNA backbone. On the other hand, the opposite ion, Cl^-, can migrate to the anode and react with hydrogenated ions but does not cause a problem due to the strong acid resistance of DNA (21).

To reduce the cost and increase the mechanical strength of the pristine gel, polysaccharides (e.g. agarose, alginate, lignin), which are widely used as in vivo skeletal materials and extracted in organisms, were combined with genomic DNA gel (22). When polysaccharides are introduced into DNA, the polymers and DNA networks form hybrid gels through intermolecular hydrogen bonds, as well as metal ion-induced chain-entangled ionic cross-linked structures. The mechanical and chemical properties and the structural morphologies of genomic DNA hybrid gels are

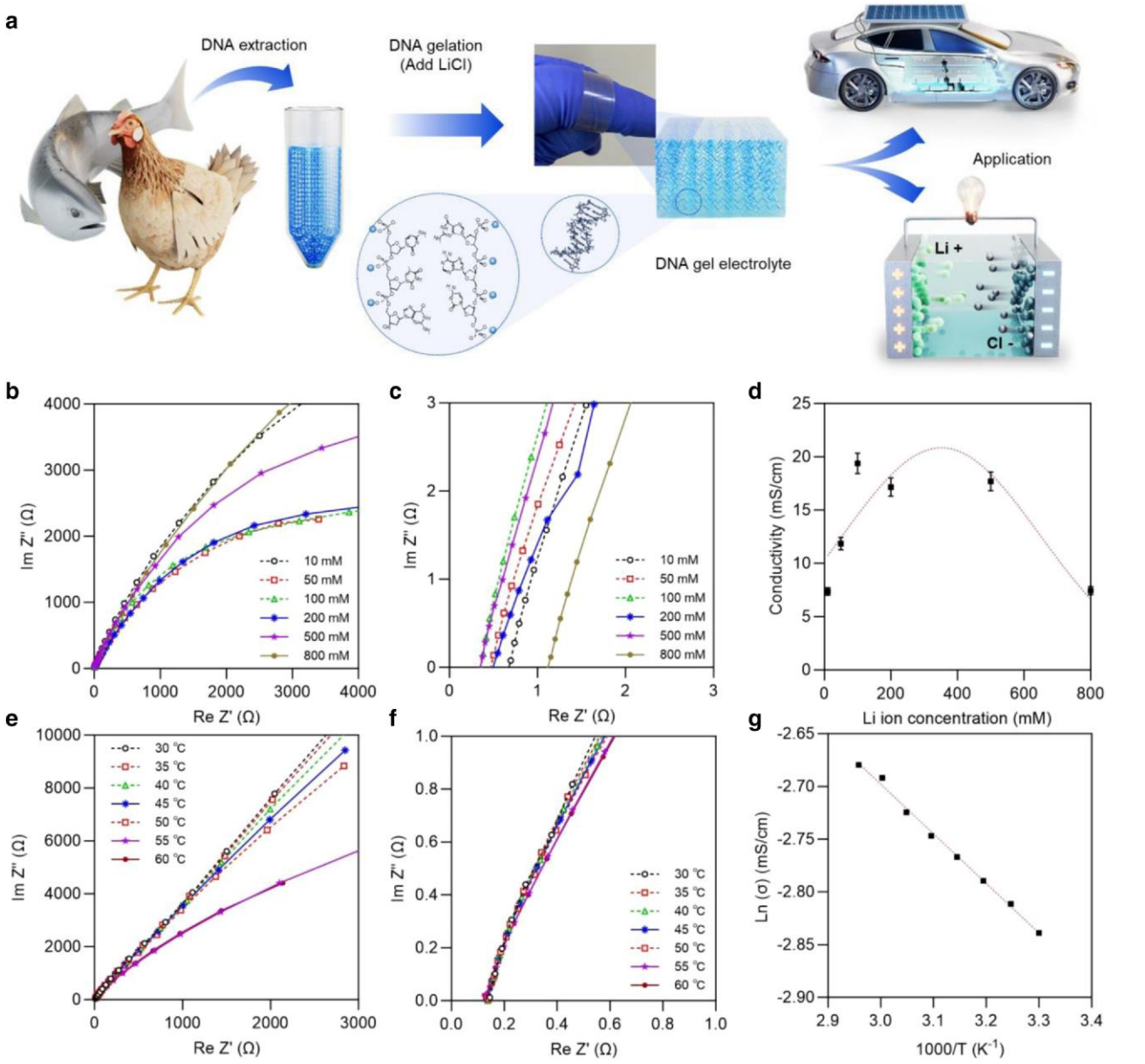

Fig. 1. A conceptual drawing of the preparation and application of biospecies-derived genomic DNA hybrid gel electrolytes and electrochemical characterization for measuring the ionic conductivity of DNA gel electrolytes. a) Power generation using gels made from DNA (or its polysaccharide mixtures) extracted from fish and birds as electrolytes. Photographic image (center) of a DNA gel wound with curling over the researcher's hand. In the schematic of the 3D polymerization network of the DNA gel electrolyte, images of model lithium ions (blue spheres) are combined in two single-stranded DNA structures. Finally, its application to electrical storage is shown with an example of vehicle driving and lighting LED bulbs. b–g) Electrochemical impedance spectroscopy (EIS) was used to determine the ionic conductivity of the DNA gel electrolyte. b, c) EIS analysis of DNA gel electrolytes with varying LiCl concentrations and Nyquist plot analysis at high frequencies, respectively. The resistance was obtained from intercepts on the real axis of the Nyquist plot, corresponding to the intrinsic bulk resistance of the DNA gel electrolyte, and evaluated the ionic conductivity for each LiCl concentration. d) Changes of the ionic conductivity with LiCl concentrations in DNA gel electrolytes. e, f) EIS analysis of DNA gels of 200 mM LiCl at different temperatures. The resistance and conductivity of DNA gel electrolytes at various temperatures were obtained from the Nyquist plot. Figure f represents a Nyquist graph at high frequency. g) Temperature-dependent ionic conductivity of the DNA gel optimized with 200 mM LiCl shown in the Arrhenius plot.

shown in Figs. 2 and S1–S3. The photographic images of a universal tensile instrument revealing the mechanical properties of DNA hybrid gels without and with PEGDA crosslinkers were shown in Fig. 2a and e, respectively. The DNA concentration is a critical parameter for studying the mechanical properties of gels due to the excellent physical entanglement and ion coordination properties. Furthermore, the tensile behavior of DNA hybrid gels was highly dependent on the choice of polysaccharides and their combinations. The stress–strain curves of DNA hybrid gels without and with PEGDA crosslinkers were displayed in Fig. 2b and f, respectively. In comparison to pure DNA gels, the elastic values of the hybrid gels were about 3-, 4-, and 2-times higher in the A/D, SA/D, and L/D hybrid gels, respectively. The DNA hybrid gels physically crosslinked by hydrogen bonding and coordination of metal ions had improved mechanical strength compared to conventional gels. The well-distributed physical entanglement effectively disperses energy from postelongation and prevents cracking thus, resulting in enhanced mechanical properties (23–26). Moreover, the

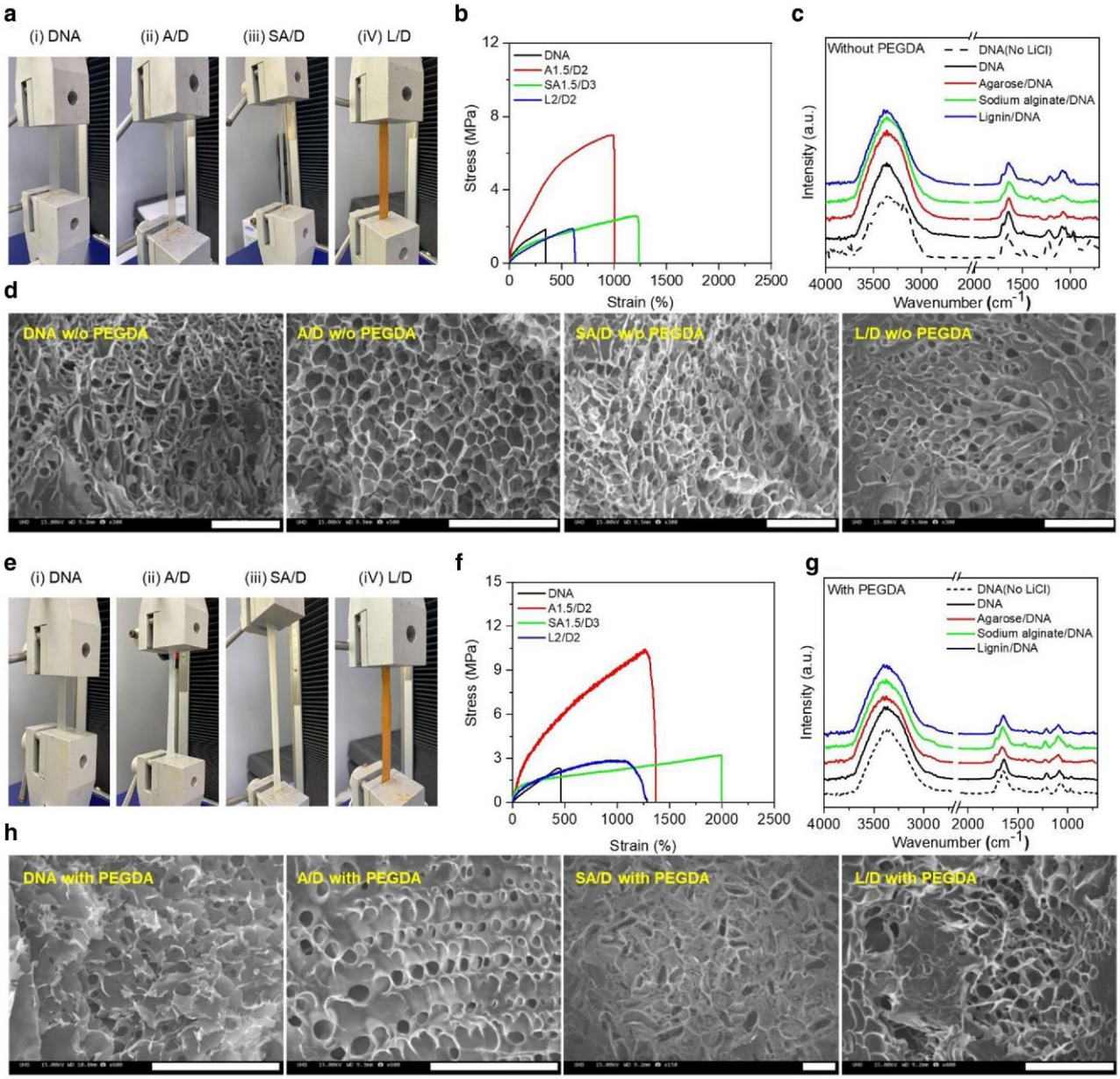

Fig. 2. Mechanical and structural properties of genomic DNA hybrid gel electrolyte without and with PEGDA cross-linkers. In a, b, e, and f, tensile stress–strain profiles of pure DNA gel and DNA hybrid gels with and without PEGDA cross-linkers were obtained along with the tensile strength measurement photographs of the DNA gels. The tensile properties shown are based on the highest ionic conductivity obtained for a selective combination of polymer and DNA concentrations: the ratio of polysaccharide to DNA was optimized to 1.5/2 for agarose/DNA (A/D), 1.5/3 for sodium alginate/DNA (SA/D), and 2/2 for lignin/DNA (L/D). The A1.5/D2, SA1.5/D3, and L2/D2 gels without PEGDA were compared to pristine genomic DNA gels (1.85 MPa, 346.22%), where the maximum tensile strengths were 6.98, 2.58, and 1.89 MPa, and the minimum elongations were 997.42, 1,235.17, and 608.03%, respectively. Compared to PEGDA-cross-linked DNA (2.6 MPa and 172.48%), A1.5/D2, SA1.5/D3, and L2/D2 hybrid gels showed significant tensile properties with maximum tensile strengths of 10.42, 3.22, and 2.84 MPa and elongations of 1,269.31, 1,994, and 1,067.41%, respectively. In c and g, there are FT-IR spectra of pure DNA (without and with LiCl) and DNA hybrid gels with and without PEGDA cross-linkers. The spectral properties were used to evaluate the corresponding band assignment and peak shift of chemical bonds and functional groups. Initially, the structure of DNA gels without LiCl was identified by FT-IR spectroscopy. All samples showed absorption bands in the spectral range of 3,000–3,700 cm^{-1}, corresponding to O–H stretching vibrations. In d and h, the external morphology of the pure DNA gels and DNA hybrid gels with or without PEGDA cross-linkers was observed using FE-SEM. A highly porous gel matrix was observed in all samples. The scale bar in the images is 100 μm.

introduction of poly(ethylene glycol) diacrylate (PEGDA) as a cross-linker in these combinations provides improved mechanical strength. Compared to the PEGDA-crosslinked pure DNA hydrogels, the hybrid gels showed approximately 7-, 11-, and 6-times higher stretchability for the A/D, SA/D, and L/D hybrid gels, respectively (Fig. 2f).

Structural properties and interactions between ionic groups and salt ions in the polymer chain of genomic DNA hybrid gels with PEGDA were investigated using FT-IR and Raman spectroscopic techniques (Figs. 2c, g and S4–S6; Table S1). The vibrational peak of the phosphate (PO^{2-}) group shifted to a lower wavenumber and the absorption intensity decreased with the introduction of lithium salt, indicating that Li^{+} has a higher affinity for the phosphate group of DNA. Typical absorption peaks of DNA were also exhibited (Table S1). For the A/D hybrid gel (without PEGDA), the FT-IR spectra are shown in Fig. 2c, and the absorption

peaks observed at approximately 1,357 cm^{-1} and 1,147 cm^{-1} confirmed hybrid gel formation and complexation between agarose and DNA due to $-CH_3$ bond bending and C–O–C bond stretching of the ether group of the agarose matrix. The peak at 1,643 cm^{-1} disappeared from the A/D hybrid gel due to C=O stretching in the carbonyl group of DNA, which confirmed that agarose successfully complexed with the DNA network. This characteristic absorption peak shift and peak formation led to the identification of hybrid gels and complexation between polymers. When PEGDA cross-linkers were used, changes in the molecular structure were similarly observed (Fig. 2g). The peak at 811 cm^{-1} corresponds to the C–H bending vibration of $-C{=}CH_2$ of PEGDA, which was not observed in pristine DNA without PEGDA, whereas it was detected at 823 cm^{-1} in pristine DNA with PEGDA. It is noted that the amine group of the guanine base of DNA has the highest nucleophilic activity, which results in the pairing of the carbon–carbon double bonds of the acrylate in PEGDA. The shift of the IR absorption peak indicates that PEGDA formed covalent bonds and was cross-linked with DNA (27). In the Raman spectra (Figs. S4–S6), the solvating structure of pure DNA gels was interpreted in DNA–Li^+ interaction studies (20). The solvation structure of DNA gel electrolytes can be explained with the polymer–cation interaction studies of DNA and lithium ions (Li^+). Typically, the ionic conduction in DNA gel electrolytes arises from the segmental motion of DNA polymer chains associated with lithium ions in the amorphous region. In order to confirm the amorphous nature of our hybrid gel electrolytes, we performed XRD analysis for the hybrid gels without and with PEGDA as illustrated in Fig. S7. An efficient coordination between oxygen atoms of phosphate groups (PO^{2-}) in DNA and Li+ stimulates ion migration, consequently displaying higher ionic conductivity. In addition, when polysaccharide was mixed with DNA, the main group of vibrations was still observed (Fig. S6). Similar to the FT-IR results, the phosphate peak of the DNA hybrid gel was merged with the polysaccharide peak and decreased. In addition, stretching vibrations due to the redshift of the O–H binding by the complex of DNA and polysaccharides were observed. The main Raman peaks of the PEGDA cross-linker were also observed at 1,242 cm^{-1}, 1,408 cm^{-1}, 1,470 cm^{-1}, 1,635 cm^{-1}, and 1,723cm^{-1}, which correspond to C–O stretching, C–OH, C–OH, C=C stretching, and –COOH bending vibrations, respectively (Fig. S6) (28). The intensity ratio was clearly reduced, and shifts were also observed at 1,640 cm^{-1} and 1,708cm^{-1}. This observation showed the formation of covalent and cross-linked acrylate groups on DNA functional groups at 1,675 cm^{-1}, which is attributed to C=O stretching vibrations. Raman spectral peak shifts and intensity changes were clearly shown in spectral studies of DNA hybrid gels with PEGDA. These were related to the formation of polymer and DNA complexes through intermolecular hydrogen bonding. In addition, the FE-SEM images showed the structural morphologies of pristine DNA and DNA hybrid gels without and with PEGDA crosslinkers as illustrated in Fig. 2d and h, respectively. It is evident that the FESEM morphologies of DNA hybrid gels exhibit interconnected and densely packed porous structures.

Electrochemical and thermal analysis of aqueous LiCl, pure DNA gel, and DNA hybrid gel as electrolytes without or with PEGDA (Figs. 3, S8, and S9, respectively) was carried out by employing cyclic voltammetry (CV), galvanostatic charge–discharge (GCD), EIS measurements, and thermal gravimetric analysis (TGA). The equivalent circuit model of EIS spectra studied with the device configuration of AC‖gel electrolyte‖AC (AC—activated carbon electrode; gel electrolyte—pristine DNA and DNA hybrid gel electrolytes) was displayed in Fig. 3a. The photographic images of aqueous LiCl (aq. LiCl), pure DNA (pristine), A/D, SA/D, and L/D, were shown in Fig. 3b, f, j, n, and r respectively. From GCD and CV curves, typical rectangular and triangular shapes were observed over a voltage range of 1.2 V for aq. LiCl and pure DNA gel and 1.5 V for DNA hybrid gel electrolytes imply the existence of a nearly ideal electrochemical double layer capacitor (EDLC) function (29). The capacitance is ascribed to the accumulation of ions between the electrode and electrolyte interface. It resulted in a high current for the hybrid gel compared to aqueous electrolyte and pure DNA gel. The *iR* drops (where *i* is current and *R* is resistance) were about 0.02 V at 1 A/g for LiCl and pure DNA gel, whereas they were about 0.004, 0.005, and 0.01 V at 1 A/g for A/D, SA/D, and L/D, respectively. This was due to the low resistance of the device, good compatibility between the gel electrolyte and the electrode, and faster ion transport in the pores of the porous activated carbon on the electrode.

The electrochemical properties such as ionic conductivity and the electrochemical potential window of the DNA hybrid gel electrolyte were evaluated by electrochemical impedance spectroscopy (EIS) and linear sweep voltammetry (LSV) (Figs. 3 and S10), respectively to understand the electrochemical interface properties. In Fig. 3, a semi-circular region from the impedance plots corresponding to the charge transfer resistance was witnessed for all electrolytes; however, a large semi-circular region was observed for the pure DNA gel electrolyte due to the weaker electrode–electrolyte interface. In DNA hybrid gel electrolytes, the semi-circular region was smaller, implying a strong electrode–electrolyte interface. The resistances with higher values indicate poor permeability, whilst a lower resistance suggests better ionic diffusions. The lower resistance values were clearly observed in the case of DNA hybrid gels implying a strong electrode–electrolyte interface compared to the pure DNA gel. Figure S11 displays a FESEM cross-section image of the electrode/electrolyte interface of the porous hybrid gel, which was continuous, confirming good adhesion between the electrode and electrolyte. This structure allowed the gel to transport ion species through a continuous conducting pathway. The thicknesses of pristine DNA, A/D, SA/D, and L/D hybrid gels without PEGDA cross-linker were 108.8, 105.3, 109.5, and 107.6 µm, respectively. Consequently, the hydroxyl groups enriched in both polymers and DNA provided water affinity, a key factor in inducing interactions between the two molecules via hydrogen bonding, thus enhancing hydrogel-based electrical storage. In addition to –OH of agarose/alginate/lignin, DNA with abundant phosphate and amine groups has evolved into a 3D porous polymer network with highly continuous and dynamic conductive ion channels. In particular, the oxygen-containing polar group in the molecular chain of the polymer showed very high hygroscopicity, which led to the significant water retention characteristics of the hybrid gel. A steep vertical line at low frequencies indicating Warburg impedance was observed in DNA hybrid gels, which clearly represents faster ion diffusion at the electrode interface compared to pure DNA gels (30, 31). In addition to exhibiting intra- and intermolecular hydrogen bonding, the porous structure also delivered significant amounts of energy (32, 33). Among the hybrid geal electrolytes, the A/D hybrid gel exhibited a higher capacitance in addition to the highest ionic conductivity (Fig. S10). The interaction between negatively charged groups in polymers and solvated metal ions can modulate the solvation structure which in result promotes migration behavior and hence facilitates an effective ion transfer and reversible ion adsorption and desorption. Hydrogel swelling studies were conducted on DNA hybrid gels with or without PEGDA cross-linkers to evaluate water uptake and porosity as shown in Fig. S12. The ion transport mechanisms of DNA hybrid gels were further investigated by temperature-dependent ionic

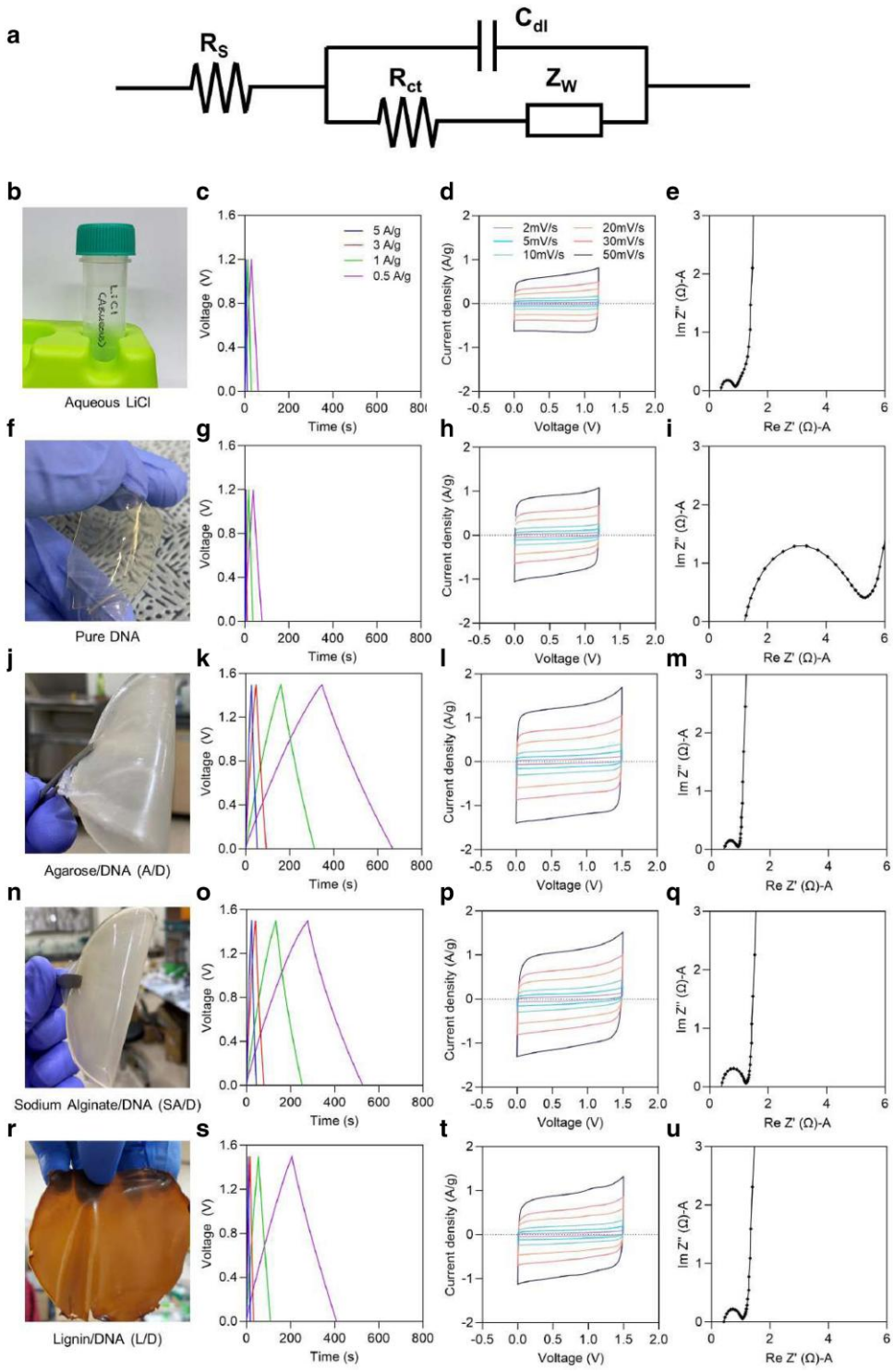

Fig. 3. Electrochemical performance and analysis of genomic DNA hybrid gels. Impedance studies were conducted in the frequency range of 100 to 1 MHz by applying an AC potential with an amplitude of 10 mV. The intercept point in the high-frequency range on the real axis represents the resistance of the electrolyte and the internal resistance of the electrode, also called the bulk resistance, and the diameter of the semicircle is attributed to the charge transfer resistance. a) Equivalent circuit of EIS spectra with the device configuration of AC‖gel electrolyte‖AC (AC—Activated Carbon electrode; gel electrolyte—pristine DNA and DNA hybrid gel electrolytes). R_s is series bulk resistance, R_{ct} is charge transfer resistance, C_{dl} is double layer capacitance, and Z_w is Warburg impedance. b, f, j, n, r) Photographic images of pristine and various DNA hybrid gels. c–e, g–i, k–m, o–q, and s–u) GCD, CV, and EIS curves of aqueous LiCl (200 mM), pure DNA gel, agarose/DNA (A/D), sodium alginate/DNA (SA/D), and lignin/DNA (L/D) hybrid gels with 200 mM LiCl without PEGDA, respectively. All GCD and CV curves were measured with different current densities ranging from 5 to 0.5 A/g and scan rates of 2 to 50 mV/s, respectively. The current density was obtained by dividing the total current by the mass of the two activated carbon electrodes. The GCD profiles and CV curves of the LiCl aqueous solution and the pure DNA gel were obtained from a potential window of 1.2 V, whereas those of the hybrid gels were obtained from a potential window of 1.5 V. In e, i, m, q, and u, they represent the Nyquist plot of the high-frequency region. Hydrogels that do not use PEGDA cross-linkers showed strong ionic conductivity, making them more efficient electrolyte materials for high-performance energy storage devices. The hydrophilic groups (–OH) and ether groups (–O–), which are abundant in agarose, can interact with aqueous electrolytes and provide many ion migration sites and high ionic conductivity, leading to significant specific capacitance.

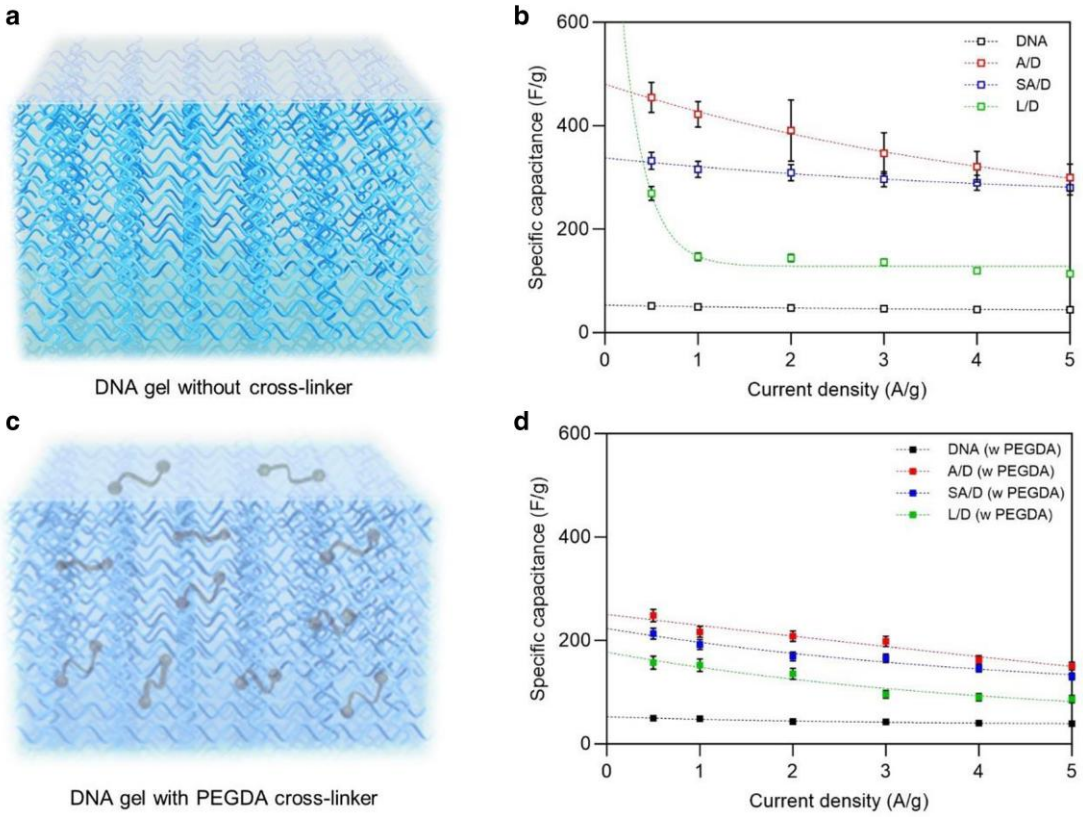

Fig. 4. Specific capacitance of genomic DNA hybrid gel supercapacitors. a to d) The specific capacitance comparisons of pure DNA, agarose/DNA (A/D), sodium alginate/DNA (SA/D), and lignin/DNA (L/D) hybrid gel electrolyte SC (200 mM of LiCl) compared at different current densities (0.5 to 5 A/g) with and without PEGDA crosslinkers, respectively. The C_{sp} values of A/D, SA/D, and L/D hybrid gels using PEGDA crosslinkers were 216.98, 192.34, and 142.48 F/g, respectively, at a current density of 1 A/g, compared to pure DNA gel SC using PEGDA (48.67 F/g).

conductivities measured at temperatures ranging from 25 to 80°C (Fig. S13). Agarose polymers can form rich interconnected submicrometer pores (400–500 nm single pore size) with high-water retention capacity.

A schematic of DNA gel without and with PEGDA cross-linker and the specific capacitance (C_{sp}) as a function of current density ranging from 0.5 to 5 A/g is illustrated in Fig. 4. The PEGDA-free A/D, SA/D, and L/D hybrid gel-based supercapacitors (SCs) exhibited specific capacitances of 425, 320, and 150 F/g, respectively at 1 A/g, which clearly demonstrates the superior performance of the hybrid gel compared to the pure DNA gel SC, which showed a specific capacitance of 50 F/g. The C_{sp} of all SCs tended to decrease monotonically with increasing current density due to a decrease in the polarization concentration at the electrode/electrolyte interface. In addition, C_{sp} of the hybrid gel SCs was higher than those of various EDLC SCs with various membranes such as cellulose (110 F/g), polypropylene (75.8 F/g), and polyurethane/wood composite gels (150 F/g) (25, 34, 35). The capacitances of EDLC SCs based on A/D, SA/D, and L/D at a current density of 5 A/g were 78.5%, 88%, and 77.2% at 1 A/g, respectively, indicating excellent rate capability. Figure 4d illustrates theC_{sp} values for A/D, SA/D, and L/D hybrid gels with PEGDA cross-linker were evaluated as 216.98, 192.34, and 142.48 F/g, respectively at a current density of 1 A/g, when compared to pristine DNA gel SC with PEGDA (48.67 F/g).

The long-term cycle stabilities of DNA hybrid gels using different polysaccharides were characterized by GCD measurements at a current density of 1 A/g (Fig. 5). Compared to pure DNA gels with or without PEGDA which showed cycle stabilities of 89% (and 90%) for 15,679 cycles and 85% (85%) for 14,745 cycles, respectively, PEGDA containing A/D, SA/D, and L/D all exhibited cycling stability up to 20,000 cycles with capacitance retention (Coulomb efficiency) values of 90.1% (95.5%), 87.9% (93.3%), and 88.8% (93.4%), respectively. Interestingly, PEGDA-free A/D, SA/D, and L/D hybrid gels showed higher capacity retention rates of 93.8% (99.9%), 90.9% (99.8%), and 93.5% (98.9%) along with remarkable cycle stabilities up to 180,336, 173,447, and 142,500 cycles, respectively. Detailed comparisons of DNA-hybrid gels with previously reported flexible supercapacitors were displayed in Table 1 (25, 32, 35–47). The perfectly complex DNA hybrid gel and the highly flexible nature of the polymer network can maintain its structure during the entire cycling process, so higher capacitance retention can be achieved for over 100,000 cycles. Due to an efficient electrode and electrolyte interface, a stable capacitance for longer cycles was witnessed which was ascribed to lower interface resistance and faster ion transport in the pores of the activated carbon electrode. To reinforce the above results, the voltage (iR) drop with respect to cycle number was plotted for DNA hybrid gels without and with PEGDA as displayed in Fig. S14a. The voltage drop was significantly higher in case of pristine DNA gels (higher when PEGDA is introduced) and perceived a lower voltage drop for A/D hybrid gels without PEGDA. The abundant active hydroxyl groups and uniform pore structure in DNA hybrid gels play a very important role in electrolyte retention, mechanical properties, and ion transport, improving the capacitance cycle stability. Key parameters such as energy and power densities were calculated to evaluate the performance of energy storage devices and were compared with previously reported supercapacitors. Figure 6a

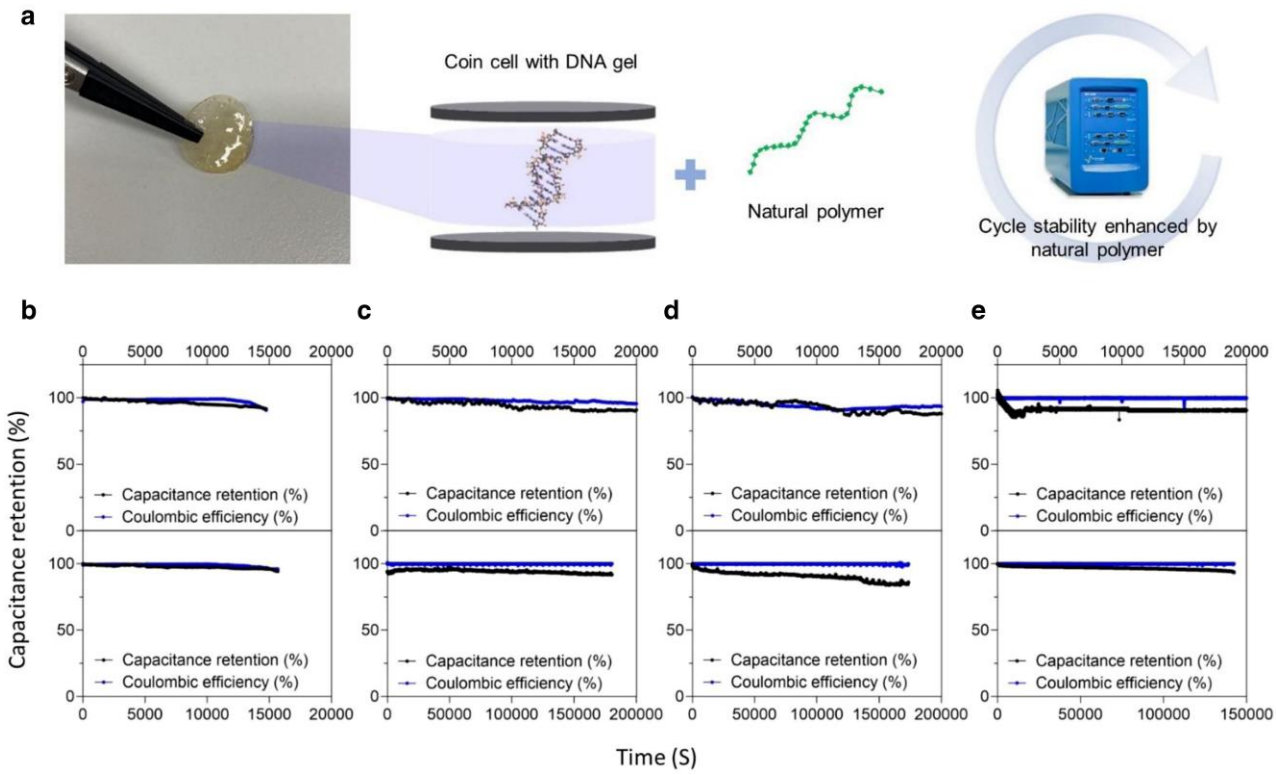

Fig. 5. Long-term cycle stability indicating capacitance retention and coulombic efficiency of genomic DNA hybrid gels using 200 mM of LiCl with or without PEGDA cross-linkers. a) Image snapshot of circular DNA-carbohydrate hybrid gel mounted between coin cells; it showed improved cycle stability by DNA gel mixed with carbohydrate polymers. b–e) The electrochemical cycling of pure DNA, A/D, SA/D, and L/D gel SC (200 mM LiCl) with and without PEGDA cross-linkers was studied at a current density of 1 A/g. Furthermore, the cyclic stability and retention properties of the DNA hybrid gel with PEGDA were not significantly high. This can be attributed to the tightly packed structure with the introduction of cross-linkers, which reduces porosity and decreases polymer network space, blocking ions passing through the gel electrolyte during the charging/discharging process. For 180,336 cycles, the device had a much better capacitance retention rate of 93.8% than other devices including P(DMAEMA-PEGMA) (PDPA) (72.89%). The low cycling performances of pure DNA gels may be due to the decomposition of the gel during continuous charging and discharging.

illustrates the Ragone plot showing the DNA hybrid gel SCs achieved significant energy and power densities owing to their high ionic conductivities and good electrode/electrolyte interface compared to those previously reported hydrogel supercapacitors (48–53). Previous reports explored the substantial achievements of energy and power densities and the use of such materials has significantly enhanced whilst increasing their cost and complex process in addition to the limited cyclic stability (54–56).

Despite the fact that the supercapacitors result in high power density (PD) and rapid charging/discharging capabilities, they typically have lower energy densities (EDs) compared to batteries. Nevertheless, the integration of biopolymers such as DNA in supercapacitors grants an opportunity to enhance the sustainability of these devices and potentially improve their electrochemical properties. Many studies exhibit higher PDs, but relatively lower EDs and longer lifetime in electrochemical supercapacitors inhibit a wide range of applications. Consequently, different strategies have been developed and the devices with high ED and PD have allured significant attention. This could involve looking at how ED and PD vary with changes in material composition, structure, or operational parameters. However, DNA biopolymers may help to improve this metric by allowing for higher capacitance materials or by enabling novel architectures that increase the effective surface area for charge storage and provide a stable matrix for rapid ion transport.

In addition, the interface between electrode and DNA gel electrolyte plays a prime role in determining the efficiency which further enhances ED and PD. Here, the studies on EDLC behavior of DNA hybrid gels representing remarkable EDs and PDs are displayed across a broad range of cycles. A constant ED and PD were achieved for large number of cycles clearly indicates the stable electrode/electrolyte interface and low resistance (Fig. S14). The significant aggregation of ion pairs that block the ionic transportation in gel electrolytes results in declining capacitance, ED, and PD values. Our results specify that even after thousands of cycles, the stable capacitance, ED, and PD were observed, which clearly signifies that the proper ion adsorption and desorption at the electrode surface as well as low internal resistance. The ED and PDs were analyzed with respect to cycle number. From the analysis, the ED of A/D (without PEGDA) at the initial cycle was 28.11 Wh/kg (@ 2 A/g), and as the cycle number increases to 100, the ED displays a constant 27.98 Wh/kg, further resulting to 27.9 Wh/kg at expanded 100,000 cycles, which was so consistent and higher than the previously reported bio polymer electrolytes (46, 47). Similarly, the PD of A/D (without PEGDA) at the initial cycles was 142.4 kW/kg, whereas at 100 cycles the PD is 138.88 kW/kg (constant trend), followed by 130.81 kW/kg at 100,000 cycles, which resulted in only 8% reduction even after prolonged cyclic stability. These stable and consistent ED and PD values indicate the superior electrochemical performances owing to the greater electrode–electrolyte interface and have potential to be used in future EDLC devices.

The device was further employed for practical applications to exploit the exceptional electrochemical properties of the DNA hybrid gel SC (Fig. 6b–g and Videos S1–S4). DNA hybrid SC devices

Table 1. Comparisons of DNA hybrid gel supercapacitors with the previously reported flexible supercapacitors.

Material	Current density	C_{sp} (F/g)	Cycle stability (Cycle No.)	Reference
Cellulose	1 A/g	172	10000	(25)
Agarose/NaCl	1 A/g	268.1	1200	(32)
Polyurethane/ porous wood	0.5 A/g	155	4000	(35)
PAAm-PAni	2 A/g	322	50000	(36)
PVDF-HFP	2 A/g	103	2000	(37)
P(AA-co-AAm)/ $CoCl_2$	0.5 A/g	134.1	5000	(38)
(HFBA)-co-(HEMA)	1.5 A/g	45	8000	(39)
Polyacrylamide	1 mA/g	100	4000	(40)
PVA/terephthalic acid/$CoCl_2$	0.5 A/g	139.2	2000	(41)
Sodium alginate/ borax	0.25 A/g	185.3	10000	(14)
PVA/BMIMI	0.5 A/g	52.7	1000	(42)
PVA/tannic acid	5 A/g	27.6	10000	(43)
Chitosan/starch	0.5 mA/cm^2	16.1	2500	(44)
Chitosan	0.5 A/g	31.89	400	(45)
Methyl cellulose: dextran	0.2 mA/cm^2	79	100	(46)
Methyl cellulose	0.095 mA/ cm^2	100	180	(47)
Agarose/DNA	1 A/g	425	180336	This work
Alginate/DNA	1 A/g	320	173447	This work
Lignin/DNA	1 A/g	150	142500	This work

were assembled in tandem configurations to meet a wide range of operating voltages and currents (Fig. 6h–j). The CV curve with one, two, and three devices connected in series and parallel showed that the DNA hybrid gel was stable up to a potential window of 5 V (Fig. 6i). Following the CV curve, the GCD curve had an ideal triangular shape with a nearly symmetric charge–discharge curve (Fig. 6j). In contrast to a single device operating at 1.5 V, the tandem series SC represented a 3 V window for two devices and a 5 V window for three devices. In parallel assemblies, the output current increased three and five-fold for two and three devices, respectively, and the discharge time was two and four times that of a single device at the same voltage (Fig. 6i and j). The SC devices can potentially power a variety of electronic components such as LEDs, digital clocks, motors in mini cars, and motor fans. The devices were connected in series and charged with different energy sources (e.g. sun and potential difference) and applied to LEDs of different colors (can power 2 LEDs at once). The device was charged for just 1 min and remained ON for more than an hour. The performance was maintained regardless of the bending (Fig. S15). These excellent results demonstrate that the flexible genomic DNA hybrid gel electrolyte SC is a promising device for high-performance energy storage applications. The development of DNA-based bending supercapacitors has the potential to revolutionize the energy storage industry and provide good opportunities for the design of sustainable and eco-friendly energy storage devices. However, since it is in the early stages of development, more research is needed for commercialization. Research directions to be explored include: (i) a full understanding of the electrochemical properties of DNA and optimization of its performance as a next-generation energy storage material and (ii) implementation of energy density equivalent to secondary batteries and realization of higher-efficiency charging/discharging, 24–100 V high-voltage technology and about 550 V capacitive voltage.

Discussion

A flexible supercapacitor, which is valuable in many fields, is a high-power device that can store a lot of energy instantaneously by charging and discharging the energy accumulated by physical adsorption and desorption on the electrode surface and then supply high current temporarily or continuously, regardless of the physical degeneration of the appearance. To realize this, many researchers are mainly focused on making electrodes with very high specific surface areas (57, 58). Electrolytes, which are closely related to the rate of ion migration, an important variable in charge storage, have long been neglected due to the limitation of available materials even though they have tremendous value in developing supercapacitors. Presently, few polymer groups are used for this purpose, such as polyvinyl alcohol (PVA), poly(ethylene oxide) (PEO), and poly(acrylic acid) (PAA) are environmentally unfriendly and unsuitable for long-term use because gradual volatilization of water results in poor ionic conductivity, cycling instability, and electrochemical degradation (59–61). To overcome these issues, alternatives are urgently needed. There is a very efficient energy production system in vivo that we cannot imitate through the close interaction of genes with many enzymes and small molecules at isotherms (62). To implement a drivable bending supercapacitor that mimics this at various temperatures, we turned our attention to using genomic DNA hydrogel electrolytes linked to polysaccharides used as skeletal structures in vivo, excluding thermally unstable enzymes. This electrolyte demonstrated excellent mechanical resistance, a high tensile stress of 6.98 MPa, and a maximum strain of 997.42%. It is thermodynamically stable even at high voltages and is suitable for the construction of high-performance energy storage devices while offering robust water retention ability, providing ion migration channels to electrolyte ions (73.27 mS/cm) and inducing the vacating effect inside the supercapacitor (63). Moreover, the high-water retention capacity provides a robust cyclability with a capacitance retention rate of 93.8% after 180,336 cycles, maintaining a maximum energy density of 35.07 Wh/kg and a maximum power density of 193.9 kW/kg. When this supercapacitor was fully bent and subjected to a weight of 2 kg, its specific capacitance and charge/discharge behavior did not change significantly. As a result, flexible solid-state supercapacitors have been practically used in solar cells, cars, and LED lightning.

Additional features that make it more distinct from existing systems include (i) it was easy to transfer ions to the electrode surface in contact with DNA so that charging and discharging can be performed at a faster speed, and overcharging or discharging did not occur, thereby simplifying the electric circuit and reducing costs. (ii) Durability temperature characteristics in the wide range (−20–+ 90°C) are possible. (iii) The DNA electrolyte is composed of DNA, which has an inherent affinity for various metal ions including lithium ions used as a test model in this study. The conversion of lithium ions to sodium ions did not significantly deteriorate the electrical storage performance (Figs. S16–S18). (iv) The DNA and polysaccharides used have several attractive features for energy storage applications as they are biocompatible, biodegradable, abundant in nature, noncombustible, and eco-friendly. Polysaccharides such as cellulose and starch have already been used as electrolyte materials in energy storage devices (Fig. S19). (v) Combining polysaccharides and DNA can dramatically improve the performance and provide additional benefits such as improved stability and increased ionic conductivity. When salmon DNA used as a test model in electrolytes was converted into chicken or human genomic

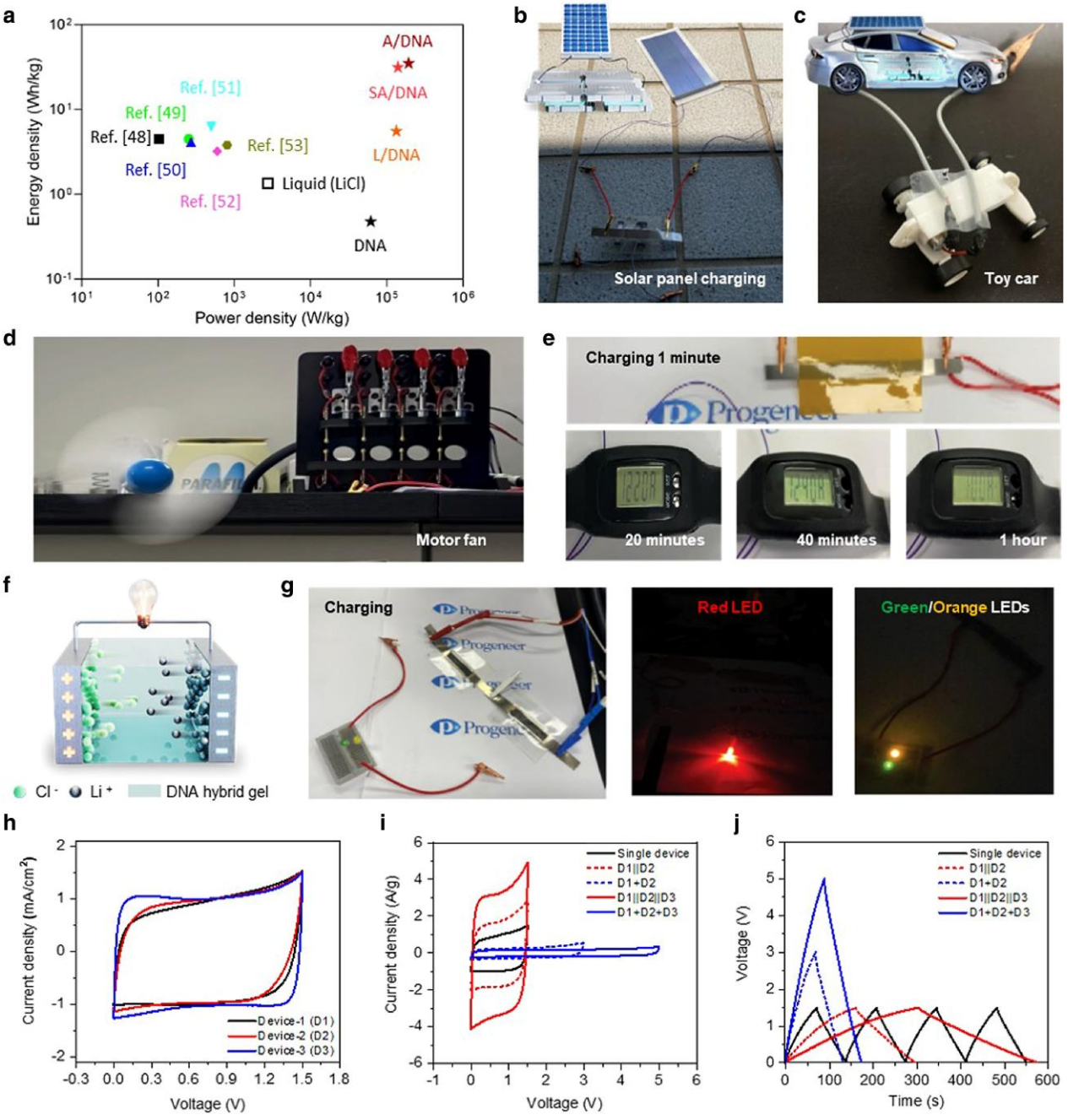

Fig. 6. Real-time application of built-in genomic DNA hybrid gel SCs in various wearable and portable electronic devices. Real-time application of DNA hybrid gel SCs embedded in different wearable and portable electronic devices. To demonstrate real-time applications, two SC devices were connected in series and parallel. a) Ragone plot of DNA hybrid gel SCs compared to previous literature using activated carbon electrodes (48–53). The performances of existing supercapacitors and genomic DNA hybrid gel SCs in terms of energy density and power density were compared. The respective maximum energy density and power density were 35.07 Wh/kg and 1.939×10^5 W/kg for the agarose/DNA hybrid gel SC, whereas, for the alginate/DNA and lignin/DNA hybrid gel SCs, the energy and power densities were 31.5 Wh/kg and 1.406×10^5 W/kg, and 5.544 Wh/kg and 1.339×10^5 W/kg, respectively. b and c) A demonstration of a self-powered charging station with a DNA hybrid gel SC as an energy storage device to power flexible solar cells and toy cars as an energy harvesting source. d) A digital image where two DNA hybrid SC devices connected in parallel power a fan. e) A digital image of a single DNA hybrid SC device continuously powering a digital clock for 1 h. f) The outline mechanism of DNA hybrid gel SC configuration. g) Real-time application of red, green, and orange LEDs powered by two SC serial connection devices charged using a potentiostat. h) CV (scan rate of 50 mV/s) of the three devices used in the applications. The SC performance was observed and compared to various single devices (D1, D2, D3). All devices exhibited typical EDLC-type behavior where the significant distribution of charge at the two electrodes was confirmed and the high reversibility of the devices was explained. i and j) The CV (@ 50 mV/s) and GCD (@ 1 A/g) curves of three devices connected in tandem configurations.

DNA, the effect on performance was negligible (Figs. S20–S24 and Tables S3–S7). It will be possible to create great value by increasing access to energy storage eco-technology and expanding the market with a wide range of interests and creative ideas for technologies that require power.

Materials and methods

Materials

Fiber-like sodium salt DNA was extracted from salmon fish (SDNA) and were supplied by GEM Corporation (Shiga, Japan).

The chemicals poly(ethylene glycol) diacrylate (PEGDA) (average Mn 700), lithium chloride (LiCl), sodium chloride (NaCl), alginic acid sodium salt (sodium alginate [SA]), lignosulfonic acid sodium salt (lignin), and *N*-methyl-2-pyrrolidone (NMP) were purchased from Sigma-Aldrich Inc. (Seoul, South Korea). Agarose was obtained from Bioneer Co., Ltd. (Daejeon, South Korea). Activated carbon powder (YP-50F), conductive carbon black, and PVDF binder were purchased from KURARAY Co., Ltd. (Tokyo, Japan). All materials were used without any further purification. The chicken and human blood samples were purchased from Innovative Research Inc. (Michigan, USA); They were provided in the form of Innovative Grade US Origin Chicken Whole Blood 50 mL and Single Donor Human Whole Blood 10 mL, respectively.

Synthesis of pure DNA gel electrolyte

The DNA gel electrolytes were synthesized using simple heating/cooling process as previously described (20). Briefly, to synthesize 3 wt.% pristine DNA gel electrolyte, 0.6 g of salmon sperm DNA was dissolved in 20 mL of deionized (DI) water with various concentrations (10 mM to 1 M) of a lithium chloride (LiCl) solution followed by stirring at 90°C (heating process) until the DNA was dissolved completely. The as-obtained aqueous DNA solution incorporating LiCl was poured into a circular Petri dish and incubated at room temperature overnight through the cooling process in which the solution solidifies (gel state) and resulting in a uniform and transparent DNA gel electrolyte. In addition, the excess water was removed by drying the obtained gels in a hot-air oven at 50°C overnight to obtain a peelable DNA gel that can be utilized for electrochemical measurements.

Hybrid gel of DNA and polysaccharides without and with PEGDA cross-linkers

The DNA-polysaccharide hybrid hydrogels were developed with both physically (without PEGDA cross-linkers) and chemically cross-linked (with PEGDA) by a single-pot synthesis method using heating/cooling process. The Agarose/DNA (simply abbreviated as A/D) hybrid hydrogel precursors include water, DNA, agarose monomer, and PEGDA cross-linker, where the gel precursor reactants were heated to a temperature higher than the melting temperature, and maintained until the polymers were in solution state. As an example, to synthesize A1.5/D2 hybrid gels without PEGDA cross-linkers, 4 wt.% of salmon sperm DNA was dissolved in 10 mL of DI water with 800 mM concentration of LiCl solution and stirred at 90°C until the DNA was completely dissolved, and 3 wt.% of Agarose powder was dissolved in 10 mL of DI water in a microwave oven. The DNA and Polysaccharides were prepared at different wt.% ratios and mixed with various combinations (such as 1:1, 1:2, 1:3, 1.5:1, 1.5:2, 1.5:3, 2:1, 2:2, 2:3, 3:1, 3:2, 3:3). The sample notations were as follows: 1 wt.% DNA and Agarose were denoted as D1 and A1, respectively. The dissolved DNA and Agarose solutions were thoroughly blended for a few hours at 90°C. Similarly, to synthesize A1.5/D2 hybrid gels with PEGDA cross-linkers, both the dissolved DNA and agarose solutions were thoroughly mixed for a few hours at 90°C, and finally 1 mL of PEGDA was added which acts as a cross-linking agent to cross-link the DNA and agarose polymers. After thorough mixing, the mixtures were poured into a circular Petri dish and were incubated at room temperature overnight, which solidified and resulted in a uniform and transparent hybrid gel electrolyte. The excess water was removed by drying the gels in a hot-air oven at 50°C overnight to obtain a peelable gel, which was utilized for electrochemical measurements.

Besides, sodium alginate/DNA (SA/D) and lignin/DNA (L/D) hydrogel samples were also prepared in the same procedure as A/D hybrid gels. Briefly, sodium alginate and lignin precursors were dissolved separately and mixed thoroughly with DNA for a few hours while heated (in the case of hybrid gel with PEGDA cross-linkers, 1 mL of PEGDA was added after thorough mixing of DNA and polymers) and cooled to room temperature followed by removing excess water at 50°C until we obtained a peelable gel. The electrochemical properties (potential stability and ionic conductivity) were evaluated using linear sweep voltammetry (LSV) and electrochemical impedance spectroscopy (EIS), respectively, for various combinations of DNA hybrid gels.

Fabrication of genomic DNA hybrid gel supercapacitors

The electrode material utilized to fabricate the supercapacitors were activated carbon electrodes (YP-50F) which were purchased from Kuraray. A symmetrical two-electrode capacitor configuration was utilized to analyze the electrochemical performance of the DNA hybrid gel SC devices. The activated carbon electrodes used for electrochemical performances were prepared as follows: a uniform slurry was prepared by mixing activated carbon powder (80%), conductive carbon black (10%), and PVDF binder (10%) with the required amount of *N*-methyl-2-pyrrolidone (NMP). Titanium substrates (0.1 mm thick and 99% purity) were used as current collectors, whereas the prepared slurry was coated with Dr. Blade on to the current collectors and cut into circular discs of an area 1.76 cm^2 which were vacuum-dried at 80°C overnight to obtain activated carbon electrodes. The activated carbon electrodes used for supercapacitor measurements have an average thickness of ~70 μm and average weight of 10 mg per electrode (with an average weight of 2.84 mg/cm^2).

The DNA gel (acting as both separator and electrolyte) (circular shaped gels with a diameter of 1.5 cm were utilized (area = 1.76 cm^2)) was sandwiched between two activated carbon electrodes and fabricated in a symmetrical coin cell (CR2032-type, Wellcos Incorporated, Korea). Moreover, the electrochemical measurements of the flexible devices were conducted by sandwiching the DNA gel electrolyte between two carbon electrodes coated on flexible titanium substrates (1 cm × 3 cm) as current collectors and hot pressing it at 80°C under 3 MPa for 10 min. The device was sealed to be air-tight using silicone tape. The experimental methods for the extraction and amplification of gene DNA from various species (e.g. salmon, chicken, human) are described in more detail in the Supporting Experimental Method.

Acknowledgments

The authors would like to express deep gratitude to Ms. Ji Soo Yuk and Mr. Rajasekaran Beniel Jones for their help in drawing, amplifying, and supplying genomic DNAs in the blood, and to the Sungkyunkwan University Research Facility Cooperative Center (SKKU CCRF) for their use of the equipment.

Supplementary Material

Supplementary material is available at *PNAS Nexus* online.

Funding

This study was conducted with the financial support of Progeneer Inc. and was co-funded by the National Research Foundation of Korea and the Ministry of Science and ICT

(2022R1A2B5B02001237). All data are included in the manuscript and/or supporting information.

Author Contributions

S.B.M. and S.H.U designed research; S.B.M., J.K., H.H.R., and S.K. performed research; S.B.M., H.H.R., S.K., Y.T.L., S.H.B., H.S.P., and S.H.U. analyzed data; and S.B.M. and S.H.U. wrote the article.

Data Availability

The data underlying this article are available in the article and in its online supplementary material.

References

1 Ding J, *et al.* 2024. Recent advances in biopolymer-based hydrogel electrolytes for flexible supercapacitors. *ACS Energy Lett*. 9(4): 1803–1825.
2 Zheng H, *et al.* 2023. Scalable fabrication of all-biopolymer-derived conductive hydrogels for flexible mechanosensors and zinc-ion hybrid supercapacitors. *ACS Appl Eng Mater*. 1(5):1375–1383.
3 Carvalho JT, *et al.* 2022. Carbon-yarn-based supercapacitors with in situ regenerated cellulose hydrogel for sustainable wearable electronics. *ACS Appl Energy Mater*. 5(10):11987–11996.
4 Salimijazi F, Parra E, Barstow B. 2019. Electrical energy storage with engineered biological systems. *J Biol Eng*. 13:38.
5 Ahn SY, Liu J, Vellampatti S, Wu Y, Um SH. 2021. DNA transformations for diagnosis and therapy. *Adv Funct Mater*. 31:2008279.
6 Hur J, *et al.* 2013. DNA hydrogel-based supercapacitors operating in physiological fluids. *Sci Rep*. 3:1–7.
7 Meng YS, Srinivasan V, Xu K. 2022. Designing better electrolytes. *Science*. 378(6624):1065.
8 Pal B, Yang S, Ramesh S, Thangadurai V, Jose R. 2019. Electrolyte selection for supercapacitive devices: a critical review. *Nanoscale Adv*. 1(10):3807–3835.
9 Xu K. 2004. Nonaqueous liquid electrolytes for lithium-based rechargeable batteries. *Chem Rev*. 104(10):4303.
10 Mosa MI, *et al.* 2017. Ultrathin graphene-protein supercapacitors for miniatured bioelectronics. *Adv Energy Mater*. 7(17):1700358.
11 Ryu W-H, *et al.* 2016. Heme biomolecule as redox mediator and oxygen shuttle for efficient charging of lithium-oxygen batteries. *Nat Commun*. 7:12925.
12 Cevik E, Gunday ST, Bozkurt A, Amine R, Amine K. 2020. Bio-inspired redox mediated electrolyte for high performance flexible supercapacitor applications over broad temperature domain. *J. Power Sources*. 474:228544.
13 Kang YJ, *et al.* 2012. All-solid-state flexible supercapacitors fabricated with bacterial nanocellulose papers, carbon nanotubes, and triblock-copolymer ion gels. *ACS Nano*. 6:6400.
14 Peng K, *et al.* 2022. Green conductive hydrogel electrolyte with self-healing ability and temperature adaptability for flexible supercapacitors. *ACS Appl Mater Interfaces*. 14(34):39404–39419.
15 Cevik E, *et al.* 2022. Scalable, quasi-solid-state bio-polymer hydrogel electrolytes for high-performance supercapacitor applications. *ACS Sustainable Chem Eng*. 10(33):10839–10848.
16 Xiang L, *et al.* 2017. Gate-controlled conductance switching in DNA. *Nat Commun*. 8:14471.
17 Lastra LS, *et al.* 2022. On the origins of conductive pulse sensing inside a nanopore. *Nat Commun*. 13:2186.
18 Li CY, *et al.* 2015. Ionic conductivity, structural deformation, and programmable anisotropy of DNA origami in an electric field. *ACS Nano*. 9(2):1420–1433.
19 Guo X, Gorodetsky AA, Hone J, Barton JK, Nuckolls C. 2008. Conductivity of a single DNA duplex bridging a carbon nanotube gap. *Nat Nanotechnol*. 3:163–167.
20 Mitta SB, Rana HH, Kim J, Park HS, Um SH. 2022. Flexible supercapacitor with a pure DNA gel electrolyte. *Adv Mater Interfaces*. 9: 2200133.
21 Kim J-M, *et al.* 2020. Ecofriendly chemical activation of overlithiated layered oxides by DNA-wrapped carbon nanotubes. *Adv Energy Mater*. 10(9):190365.
22 Oliveira JT, Reis RL. 2011. Polysaccharide-based materials for cartilage tissue engineering applications. *J Tissue Eng Regen Med*. 5(6):41–436.
23 Yan T, *et al.* 2021. Hydrogen bond interpenetrated agarose/PVA network: a highly ionic conductive and flame-retardant gel polymer electrolyte. *ACS Appl Mater Interfaces*. 13(8):9856–9864.
24 Yang J, *et al.* 2021. Antifreezing zwitterionic hydrogel electrolyte with high conductivity of 12.6 mS cm−1 at −40°C through hydrated lithium ion hopping migration. *Adv Funct Mater*. 31(18): 2009438.
25 Li L, *et al.* 2018. Flexible double-cross-linked cellulose-based hydrogel and aerogel membrane for supercapacitor separator. *J Mater Chem A*. 6:24468–24478.
26 Li L, Wu P, Yu F, Ma J. 2022. Double network hydrogels for energy/environmental applications: challenges and opportunities. *J Mater Chem A*. 10:9215–9247.
27 Wang D, *et al.* 2020. Transformation of biomass DNA into biodegradable materials from gels to plastics for reducing petrochemical consumption. *J Am Chem Soc*. 142(22):10114–10124.
28 Ermeydan MA. 2018. Modification of spruce wood by UV-crosslinked PEG hydrogels inside wood cell walls. *React Funct Polym*. 131:100–106.
29 Zhang X, *et al.* 2015. A flexible ionic liquid gelled PVA-Li2SO4 polymer electrolyte for semi-solid-state supercapacitors. *Adv Mater Interfaces*. 2(15):1500267.
30 Simotwo SK, Chinnam PR, Wunder SL, Kalra V. 2017. Highly durable, self-standing solid-state supercapacitor based on an ionic liquid-rich ionogel and porous carbon nanofiber electrodes. *ACS Appl Mater Interfaces*. 9(39):33749–33757.
31 Rana HH, Park JH, Gund GS, Park HS. 2020. Highly conducting, extremely durable, phosphorylated cellulose-based ionogels for renewable flexible supercapacitors. *Energy Storage Mater*. 25:70–75.
32 Moon WG, Kim G-P, Lee M, Song HD, Yi J. 2015. A biodegradable gel electrolyte for use in high-performance flexible supercapacitors. *ACS Appl Mater Interfaces*. 7(6):3503–3511.
33 Armelin E, Perez-Madrigal MM, Aleman C, Diaz DD. 2016. Current status and challenges of biohydrogels for applications as supercapacitors and secondary batteries. *J Mater Chem A*. 4: 8952–8968.
34 Zhao D, *et al.* 2017. High performance, flexible, solid-state supercapacitors based on a renewable and biodegradable mesoporous cellulose membrane. *Adv Energy Mater*. 7(18):1700739.
35 Hou P, *et al.* 2023. A semi-transparent polyurethane/porous wood composite gel polymer electrolyte for solid-state supercapacitor with high energy density and cycling stability. *Chem Eng J*. 454: 139954.
36 Hao GP, *et al.* 2014. Stretchable and semitransparent conductive hybrid hydrogels for flexible supercapacitors. *ACS Nano*. 8: 7138–7146.
37 Chen G, Zhang F, Zhou Z, Li J, Tang Y. 2018. A flexible dual-ion battery based on PVDF-HFP-modified gel polymer electrolyte with excellent cycling performance and superior rate capability. *Adv Energy Mater*. 8:1801219.

38 Dai L, *et al.* 2019. Highly stretchable and compressible self-healing P(AA-co-AAm)/CoCl2 hydrogel electrolyte for flexible supercapacitors. *ChemElectroChem*. 6:467–472.

39 Wang J, *et al.* 2021. Flame-retardant, highly conductive, and low-temperature-resistant organic gel electrolyte for high-performance all-solid supercapacitors. *ChemSusChem*. 14:2056.

40 Liu S, *et al.* 2022. Conductive double-network hydrogel electrolytes for durable and flexible supercapacitors. *ACS Appl Mater Interfaces*. 14(13):15641–15652.

41 Ma X, *et al.* 2022. A multifunctional organogel polyelectrolyte for flexible supercapacitors. *ACS Appl Energy Mater*. 5(8):9303–9308.

42 Ma S, Xu X, Wu W. 2022. Dual-aspect expanding electrochemical characteristics of flexible supercapacitors via an ionic liquid and a high-boiling-point solvent. *ACS Appl Energy Mater*. 5(3):3401–3408.

43 Zhang J, *et al.* 2023. A supramolecular gel polymer electrolyte based on poly(vinyl alcohol) and tannic acid for flexible electrical double layer capacitors. *J Energy Storage*. 72:108618.

44 Abdulwahid RT, Aziz SB, Kadir MFZ. 2023. Environmentally friendly plasticized electrolyte based on chitosan (CS): potato starch (PS) polymers for EDLC application: steps toward the greener energy storage devices derived from biopolymers. *J Energy Storage*. 67:107636.

45 Yang H, Ji X, Tan Y, Liu Y, Ran F. 2019. Modified supramolecular carboxylated chitosan as hydrogel electrolyte for quasi-solid-state supercapacitors. *J Power Sources*. 441:22717.

46 Aziz SB, *et al.* 2020. Fabrication of high performance energy storage EDLC device from proton conducting methylcellulose: dextran polymer blend electrolytes. *J Mater Res Technol*. 9(2):1137–1150.

47 Aziz SB, *et al.* 2024. Steps towards the ideal CV and GCD results with biodegradable polymer electrolytes: plasticized MC based green electrolyte for EDLC application. *J Energy Storage*. 76:109730.

48 Liu Y, *et al.* 2015. Highly flexible freestanding porous carbon nanofibers for electrodes materials of high-performance all-carbon supercapacitors. *ACS Appl Mater Interfaces*. 7(42):23515–23520.

49 Miao F, *et al.* 2016. Polyaniline-coated electrospun carbon nanofibers with high mass loading and enhanced capacitive performance as freestanding electrodes for flexible solid-state supercapacitors. *Energy*. 95:233–241.

50 Bo J, *et al.* 2018. Morphology-controlled fabrication of polypyrrole hydrogel for solid-state supercapacitor. *J. Power Sources*. 407: 105–111.

51 Zhang W, *et al.* 2018. N/S co-doped three-dimensional graphene hydrogel for high performance supercapacitor. *Electrochim Acta*. 278:51–60.

52 Park JH, Rana HH, Lee JY, Park HS. 2019. Renewable flexible supercapacitors based on all-lignin-based hydrogel electrolytes and nanofiber electrodes. *J Mater Chem A*. 7(28):16962–16968.

53 Jeong HT, Du JF, Kim YR, Raj CJ, Kim BC. 2019. Electrochemical performances of highly stretchable polyurethane (PU) supercapacitors based on nanocarbon materials composites. *J Alloys Compd*. 777:67–72.

54 Dai J, *et al.* 2023. Mos2@polyaniline for aqueous ammonium-ion supercapacitors. *Adv Mater*. 35:2303732.

55 Lu W, *et al.* 2023. Phosphorus-mediated local charge distribution of N-configuration adsorption sites with enhanced zincophilicity and hydrophilicity for high-energy-density Zn-Ion hybrid supercapacitors. *Small*. 19:2302629.

56 Qiu Z, *et al.* 2023. Highly redox-active oligomers between graphene sheets as ultrahigh capacitance/rate and stable electrodes for supercapacitors. *Energy Storage Mater*. 60:102824.

57 Kumar L, Boruah PK, Das MR, Deka S. 2019. Superbending (0–180°) and high-voltage operating metal-oxide-based flexible supercapacitor. *ACS Appl. Mater. Interfaces*. 11(41): 37665–37674.

58 Benzigar MR, Dasireddy VDBC, Guan X, Wu T, Liu G. 2020. Advances on emerging materials for flexible supercapacitors: current trends and beyond. *Adv Funct Mater*. 30(40):2002993.

59 Li Q, *et al.* 2010. Application of poly(acrylic acid-g-gelatin)/polypyrrole gel electrolyte in a flexible quasi-solid-state dye-sensitized solar cell. *Electrochim Acta*. 55(8):2777–2781.

60 Wang SH, Hou SS, Kuo PL, Teng H. 2013. Poly(ethylene oxide)-co-poly(propylene oxide)-based gel electrolyte with high ionic conductivity and mechanical integrity for lithium-ion batteries. *ACS Appl Mater Inter*. 5(17):8477–8485.

61 Anothumakkool B, *et al.* 2016. High-performance flexible solid-state supercapacitor with an extended nanoregime interface through in situ polymer electrolyte generation. *ACS Appl Mater Inter*. 8(2):1233–1241.

62 Dagdeviren G, Li Z, Wang ZL. 2017. Energy harvesting from the animal/human body for self-powered electronics. *Annu Rev Biomed Eng*. 19:85–108.

63 Noh C, Jung YJ. 2019. Understanding the charging dynamics of an ionic liquid electric double layer capacitor via molecular dynamics simulation. *Phys Chem Chem Phys*. 21:6790–6800.